We are IntechOpen,
the world's leading publisher of
Open Access books
Built by scientists, for scientists

6,900
Open access books available

186,000
International authors and editors

200M
Downloads

154
Countries delivered to

Our authors are among the

TOP 1%
most cited scientists

12.2%
Contributors from top 500 universities

CLARIVATE ANALYTICS

BOOK CITATION INDEX

INDEXED

WEB OF SCIENCE™

Selection of our books indexed in the Book Citation Index
in Web of Science™ Core Collection (BKCI)

Interested in publishing with us?
Contact book.department@intechopen.com

Numbers displayed above are based on latest data collected.
For more information visit www.intechopen.com

Sharp Wave Based HHT Time-frequency Features with Transmission Error

Chin-Feng Lin[1], Bing-Han Yang[1], Tsung-Ii Peng[2],
Shun-Hsyung Chang[3], Yu-Yi Chien[2], and Jung-Hua Wang[1]
[1]Department of Electrical Engineering, National Taiwan Ocean University
[2]Department of Neurological Division, Chang Cung Memorial Hospital, Keelung Branch
[3]Department of Microeletronic Engineering, National Kaohsuing Marine University
Taiwan

1. Introduction

Signal analysis is a field of study that attempts to extract information features from various physical phenomena. Fourier transform (FT), wavelet transform (WT), and Hilbert-Huang transformation (HHT) are the 3 major approaches used in signal analysis (Huang et al., 1998) (Yan & Gao, 2007). FT is a global energy-frequency distribution approach that is suitable for analyzing linear, strictly periodic, and stationary signals. In contrast, HHT is a good method for analyzing non-linear and non-stationary signals, such as those associated with wind, earthquakes, electrocardiographs (ECGs), and electroencephalograms (EEGs). This method can also used to describe the local features of dynamic signals, and illustrate the energy-frequency-time distribution of these signals. The 2 principal steps employed in HHT are empirical mode decomposition (EMD) and Hilbert spectral analysis, EMD is used to decompose local signals to finite data sets, which are referred to as intrinsic mode functions (IMFs), and Hilbert transforms (HTs) are used in conjunction with the obtained IMFs to determine the instantaneous frequencies (IFs), time-frequency-energy distributions of the local time signals. A number of studies have been performed to elucidate various aspects of signal analysis. Cohen reviewed the fundamental ideas, methods, and characteristics of the time-frequency analysis approaches employed until 1989 (Cohen, 1989). Blanco *et al.*, used the Gabor transform (GT) time-frequency analysis approach to facilitate identification of the source of epileptic seizures (Blanco et al., 1997). The GT approach is similar to the fast FT approach, but GT offers the advantage of allowing the analysis of the frequencies and their time evolution. Blanco *et al.*, adopted GT to achieve maximal concentration of the time and frequency characteristics for epilepsy and obtain accurate information on the time evolution of the frequency epileptic activity. Tzallas *et al.*, used short-time Fourier transform and 12 different time-frequency distributions for studying epilepsy classification problems and discussed the obtained sensitivity, accuracy, and selectivity results, and the characteristic data features for the detection of epilepsy (Tzallas et al., 2009). However, they did not use the HHT-based time-frequency analysis approach to define epileptic sharps. Sharabaty *et al.*, used the HHT signal-analysis approach to determine the alpha and theta localizations for estimation of the vigilance level, and

proposed an alpha/theta localization algorithm for EEG signal analysis (Sharabaty et al., 2006). Wang *et al.*, extracted the data features from C3 and C4 EEG signals to design a Brain-Computer Interface (BCI) (Wang & Xu *et al.*, 2008). They discussed the accuracy of a classification system based on imagery-movement tasks and analyzed the average marginal spectra at electrode C3 and C4 during each imagery task. Wang *et al.*, also used HHT to automatically remove ocular artifacts in contaminated EEGs (Wang & Liu et al., 2008). The authors described EEGs contaminated with ocular artifacts, IMFs and the residual artifacts from FP2, and also elucidated the differences between the contaminated FP2 EEGs and the corrected EEGs. Further, they determined the differences between the power spectra for the corrected EEGs and the contaminated FP2 EEGs. In our previous studies, we have discussed the design concept for mobile telemedicine and chaos-based encryption mechanisms for biomedical signals (Lin & Chang et al., 2006)(Lin & Chang et al., 2007)(Lin & Chang, 2008)(Lin & Li, 2008)(Lin & Chung et al., 2008)(Lin & Chen et al., 2008)(Lin et al., 2009)(Lin, 2010)(Lin et al., Online First) (Lin, Online First) (Lin & Wang, Accept). In 3 previous studies, we have described the HHT-based time-frequency characteristics of the FP1 EEG signals recorded from normal and alcoholic observers watching a single picture and 2 different pictures (Lin et al., 2008) (Lin et al., 2010)(Lin et al., Online Book, 2010). In this paper, we analyzed the sharp and normal waves with a transmission bit error rate (BER) of 10^{-7} in the EEGs obtained for epilepsy patients. The IMFs, IFs, and the time-frequency-energy distributions of these EEG signals are studied. In section II, the concept of HHT is presented, and in section III we describe the simulation results and discuss the application of HHT in the analysis the sharp waves of EEG signals obtained from patients with epilepsy. In section IV and V, we present our discussions and conclusions, respectively.

2. Method

In the HHT temporal frequency-energy-time signal analysis technique, EMD is used to perform IMFs decomposition, and HT is used to obtain the IFs, and time-frequency-energy distributions of these EEG signals.

The following procedure is employed for analyzing the IMF using EMD:

Step 1.   initially assume $r_o = x(t)$ and i=1;

Step 2.   analyze the ith IMF;

      a.   initially assume $h_{i(k-1)} = r_i$, k=1;

      b.   analyze the local maximum and minimum for $h_{i(k-1)}$;

      c.   construct the upper-limit and lower-limit envelope for $h_{i(k-1)}$ by performing additional sampling;

      d.   calculate the-mean $m_{i(k-1)}$ of the upper-limit and lower-limit envelope for $h_{i(k-1)}$;

      e. $h_{ik} = h_{i(k-1)} - m_{i(k-1)}$;

      f.   if h_{ik} is the IMF, then $IMF_i = h_{ik}$; alternatively, refer to step (b) and consider k = k+1;

Step 3.   define $r_{i+1} = r_i - IMF_i$;

Step 4.   if r_{i+1} has at least 2 extreme values,
refer to step 2 or consider that the analysis procedure is complete and that r_{i+1} is the residual signal;

In such cases, IMF is defined by 2 conditions:

Condition 1: The difference between the crossing with zero and the local extreme value of the entire data shall be equal or the difference with 1.

Condition 2: The mean of any point is the average of the local maximum and minimum envelope.

In addition, the HHT-based time-frequency analysis scheme is performed on the basis of 4 assumptions:

Assumption 1: At least 2 extreme value for the signals, i.e. maximum and minimum values, are present.

Assumption 2: The scale size of the characteristic time is selected according to the extreme values and the temporal interval.

Assumption 3: If that the data to be analyzed have no extreme values but contain identifiable points that can be expressed as extreme points of single or multiple analyses, and accompany with an increase in the number of analyses, the maximum/minimum points gain significance.

Assumption 4: The final result should be the sum of the above stated composition. Thus, the single channel EEG wave can be defined as function $x(t)$, and function $x(t)$ can be expressed as the following empirical mode function to analyzes the IMF.

$$x(t) = \sum_{i=1}^{n} IMF_i(t) + r(t) \tag{1}$$

where, $IMF_i(t)$: the ith IMF

r(t): attribution function(residual)

Then

$$z(t) = x(t) + jy(t) = x(t) + jHT\{x(t)\} = a(t)e^{j\theta(t)}$$

HT{}:Hilbert Transformation

$$a(t) = \sqrt{x^2(t) + y^2(t)}$$

$$\theta(t) = \arctan(\frac{y(t)}{x(t)}) \tag{2}$$

Thus, the IF of a single channel EEG signal can be analyzed using the following equation:

$$f(t) = \frac{1}{2\pi}\frac{d\theta(t)}{dt} \tag{3}$$

Using the HHT-based time-frequency analysis technique, the time-frequency characteristic vector of the EEG signal for epilepsy can be acquired, and the frequency characteristics, amplitude characteristics, time-dependent temporal-spatial frequency correlation, and correlation of the EEG signal to the clinical characteristics can be analyzed. Furthermore, this approach can allow determination of statistically common and abnormal points, generalization of a standard by comparison with a normal sample, augmentation the efficiency of observation, and analysis of the HHT time-frequency-energy characteristics corresponding to sharp wave.

3. Simulation results

We have used an HHT-based time-frequency analysis to analyze the sharp waves in the EEG obtained for epilepsy. A sharp EEG signal was obtained from the T3 channel from a clinical patient presenting with epilepsy; the transmission BER of the EEG was 10^{-7}. Figure 1 and Figure 2 show the sharp and normal waves, respectively. Two hundred and fifty samples per second were used to generate the sharp and normal waves. The sharp wave was generated in the interval of 0.324 and 0.444 s, its length was 120 ms, and its amplitude was 73.63 mV. Tables 1, and 2 show the statistical characteristics of the IMFs of the sharp and normal waves, respectively; we assume that the received EEG signals had a transmission BER of 10^{-7}. The maximum amplitude of the sharp wave (76.64 uV) was larger than that of the normal wave (20.7 uV). We analyzed the IMFs, IFs, and time-frequency-energy distributions for the sharp and normal waves. Figure 3 and Figure 4 show the IMFs and residual function for the sharp and normal waves, respectively; these IMFs were obtained using EMD. In these examples, 4 IMFs and a residual function were decomposed for the sharp and normal waves. In these IMFs, the amplitudes of the sharp signals were higher than those of the normal waves. The analysis results show that the ratios of the energy of a sharp wave to its total energy for IMF3 and IMF4 were 34.55%, and 33.73%, respectively. Further, the ratios of a normal wave to its total energy for IMF4, and the residual function were 43.25%, and 37.63%, respectively. The ratio of the energy of a sharp wave to its IMF4 energy for δ (0.5 Hz-4 Hz) band was 98.4%, the similar ratio of a normal wave was 82.2%. Figure 5 and Figure 6 show the IFs corresponding to the sharp and normal waves, respectively. Tables 3 and 4 show the statistical characteristics of the IFs of the sharp and normal waves, respectively. The mean frequencies of the IFs of the normal waves were larger than those of the IFs of the sharp waves. The frequency-energy distributions corresponding to the sharp and normal waves in the IMF3, IMF4, and the residual function are shown in Tables 5, 6, and 7, respectively. From Table 5, the maximum energy of the sharp and normal waves in IMF3 appeared in the θ and δ bands, and they are 25374.79 uV^2 and 1336.66 uV^2, respectively. From Table 6, the maximum energies of the sharp and normal waves are 40853 uV^2 and 7696 uV^2, respectively, and they appeared in IMF4 in the δ bands. From Table 7, the maximum energies of the sharp and normal waves in the residual function are 14421.09 uV^2, and 7714.66 uV^2, respectively, in the δ bands. The time-frequency-energy distributions of sharp waves in IMF3, and IMF4 are listed in Table 8 and 9, respectively, while those of normal waves in IMF4, and the residual function are listed in Table 10 and 11, respectively. This is because the maximum energy distributions of sharp and normal waves are in IMF3, and IMF4, and IMF4, and the residual function, respectively. For IMF3, the energies of the sharp wave in the δ band and the interval of 0.3-0.5 s, and the θ band in the interval of 0.4-0.7 s, are 15247.30 uV^2, and 22203.43 uV^2, respectively, as shown in Table 8. The energies of IMF4 of the sharp wave in the δ band in the intervals of 0.1-0.2 s, 0.3-0.4 s, and 0.7-0.9 s are 6789.34 uV^2, 6003.27 uV^2, and 11534.98 uV^2, respectively, as shown in Table 9. In contrast, the energies of IMF4 of the normal wave in the δ band in the interval of 0-0.1 s, 0.1-0.3 s, 0.8-0.9 s, and 0.9-1 s are 1940.13 uV^2, 2554.11 uV^2, 1056.87 uV^2 and 2614.52 uV^2, respectively, as shown in Table 10. The energies of the residual function of the normal wave in the δ band in the intervals of 0.1-.0.2 s, 0.3-0.4 s, 0.5-0.6 s, and 0.7-0.9 s are 1348.84 uV^2, 1045.06 uV^2, 1229.81 uV^2, and 2307.81 uV^2, respectively, as shown in Table 11. These results indicate the distinct differences between

the time-frequency-energy distributions of sharp and normal waves with a transmission BER of 10^{-7} in the EEG for epilepsy.
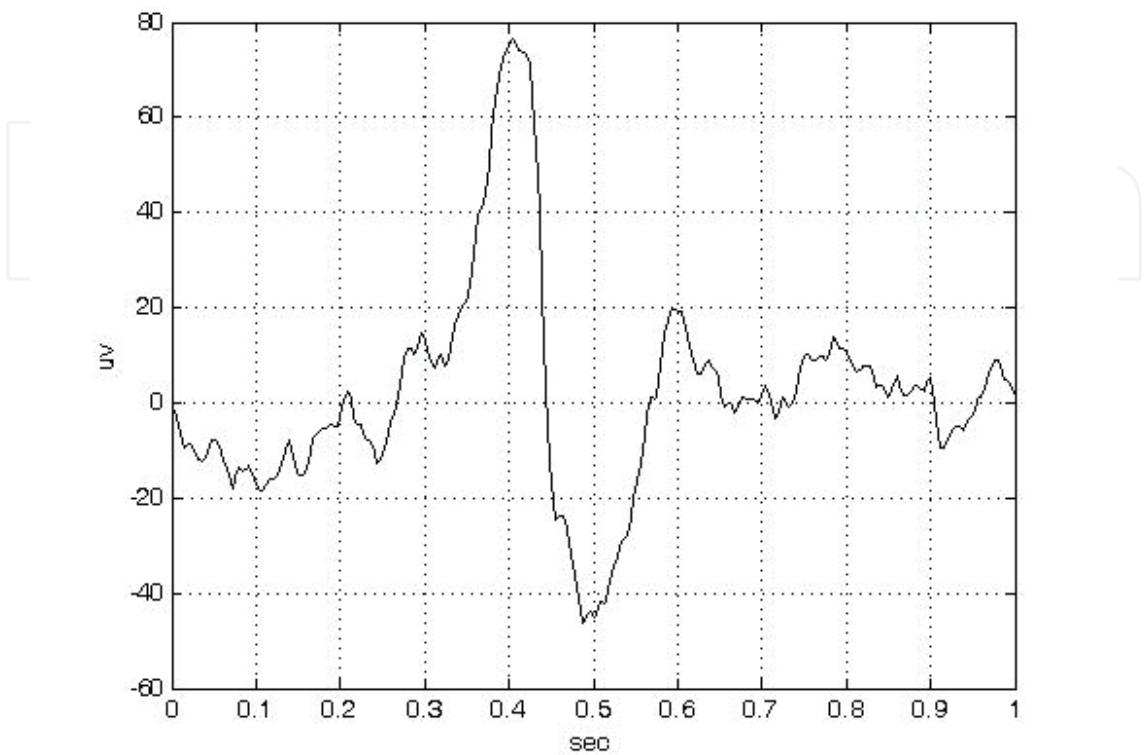

Fig. 1. Sharp wave with a transmission BER of 10^{-7}.

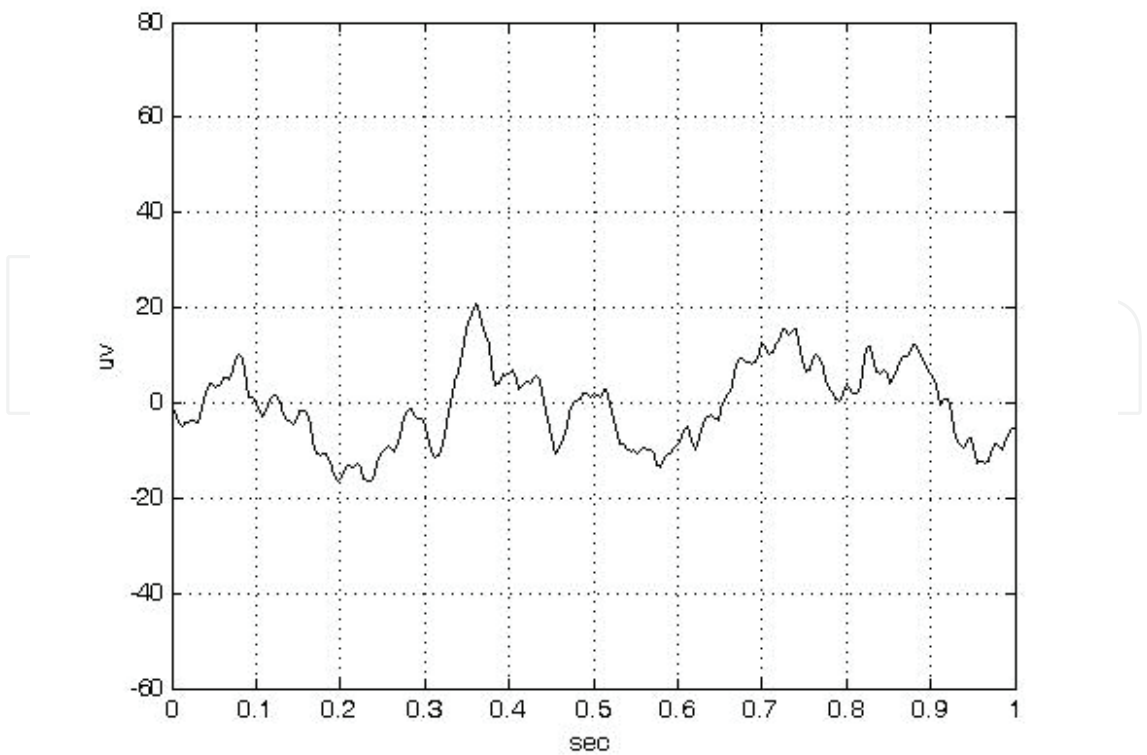

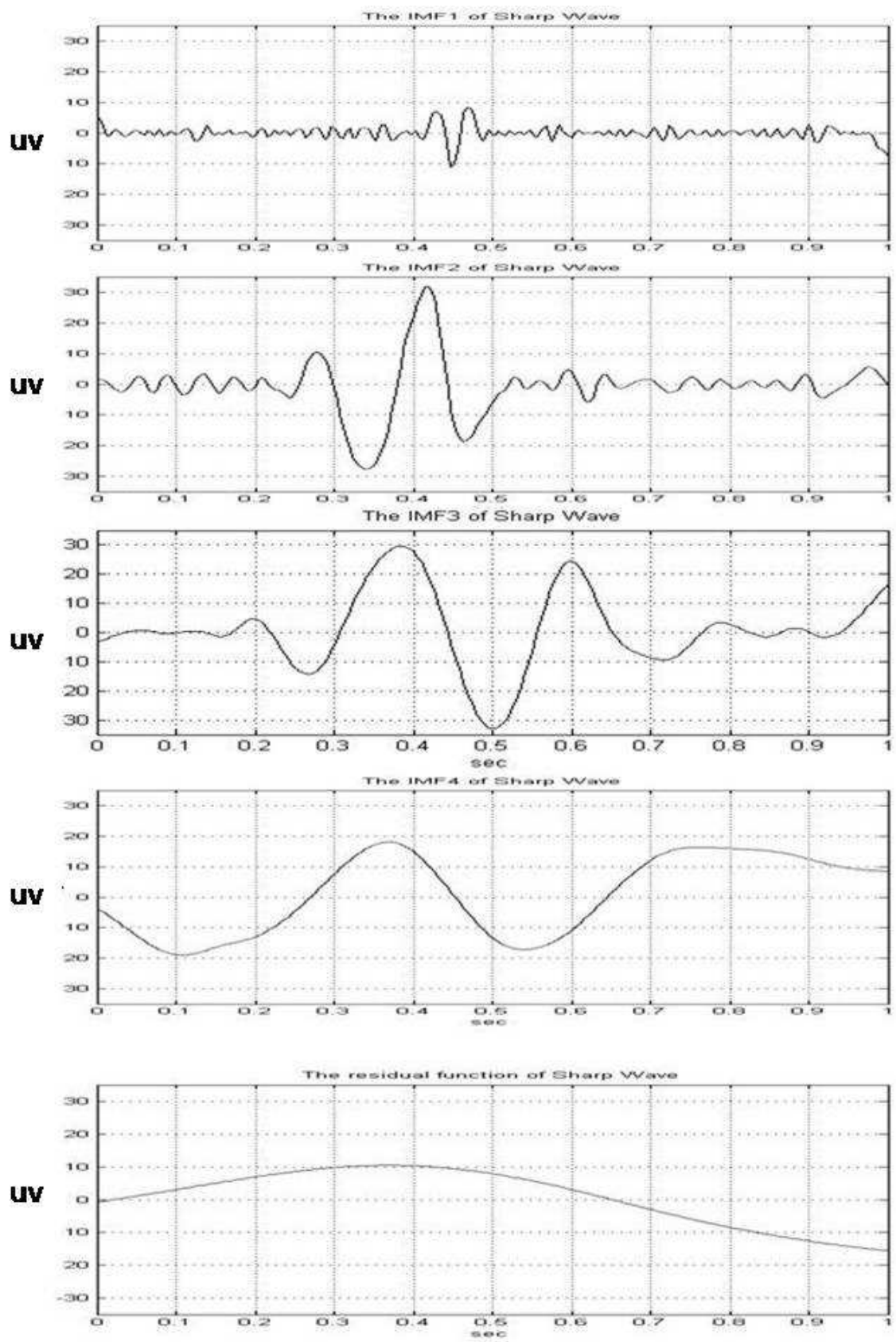Fig. 2. Normal wave with a transmission BER of 10^{-7}.

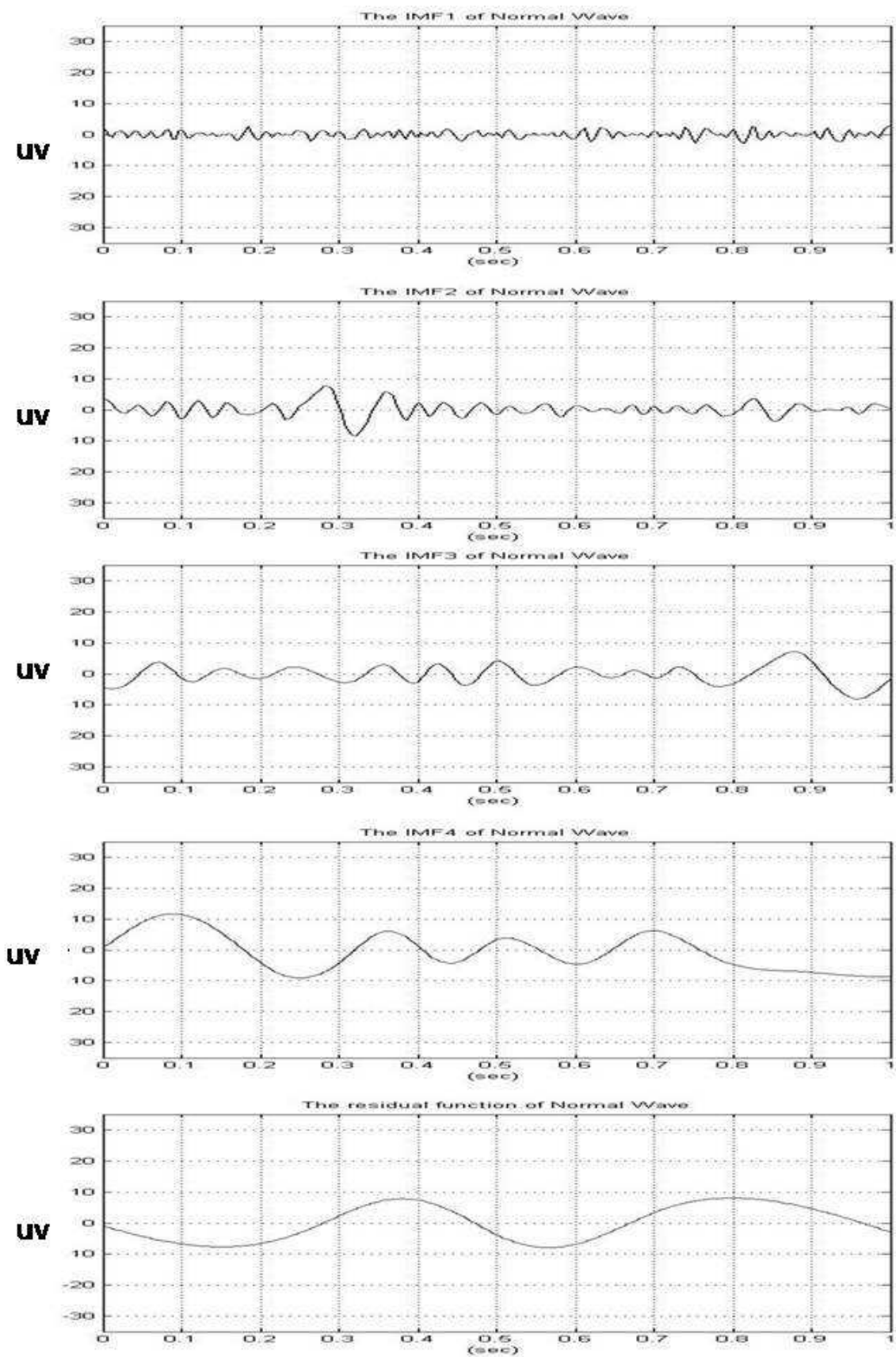Fig. 3. IMFs and the residual function of the sharp wave with a transmission BER of 10^{-7}.

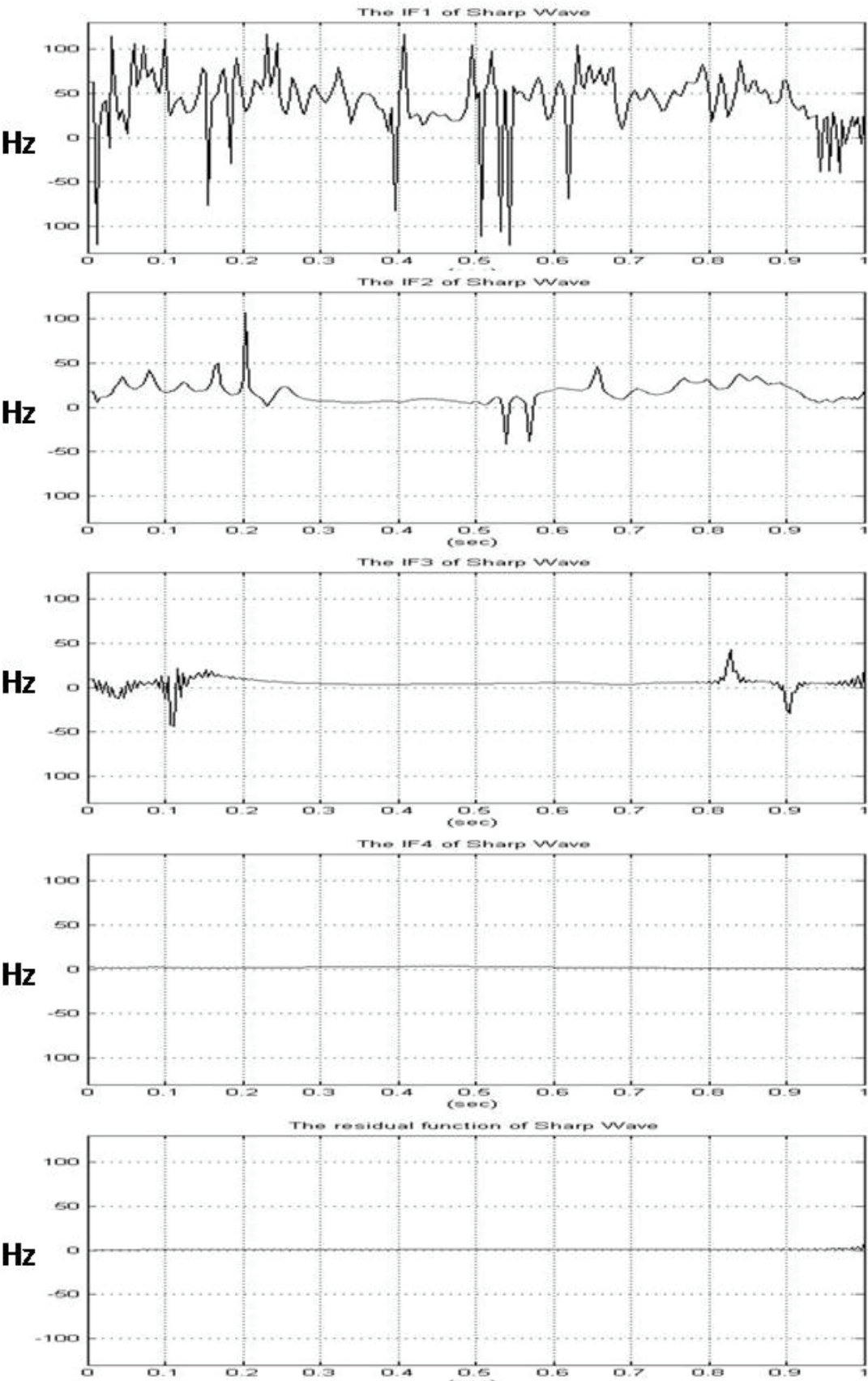Fig. 4. IMFs and the residual function of the normal wave with a transmission BER of 10^{-7}.

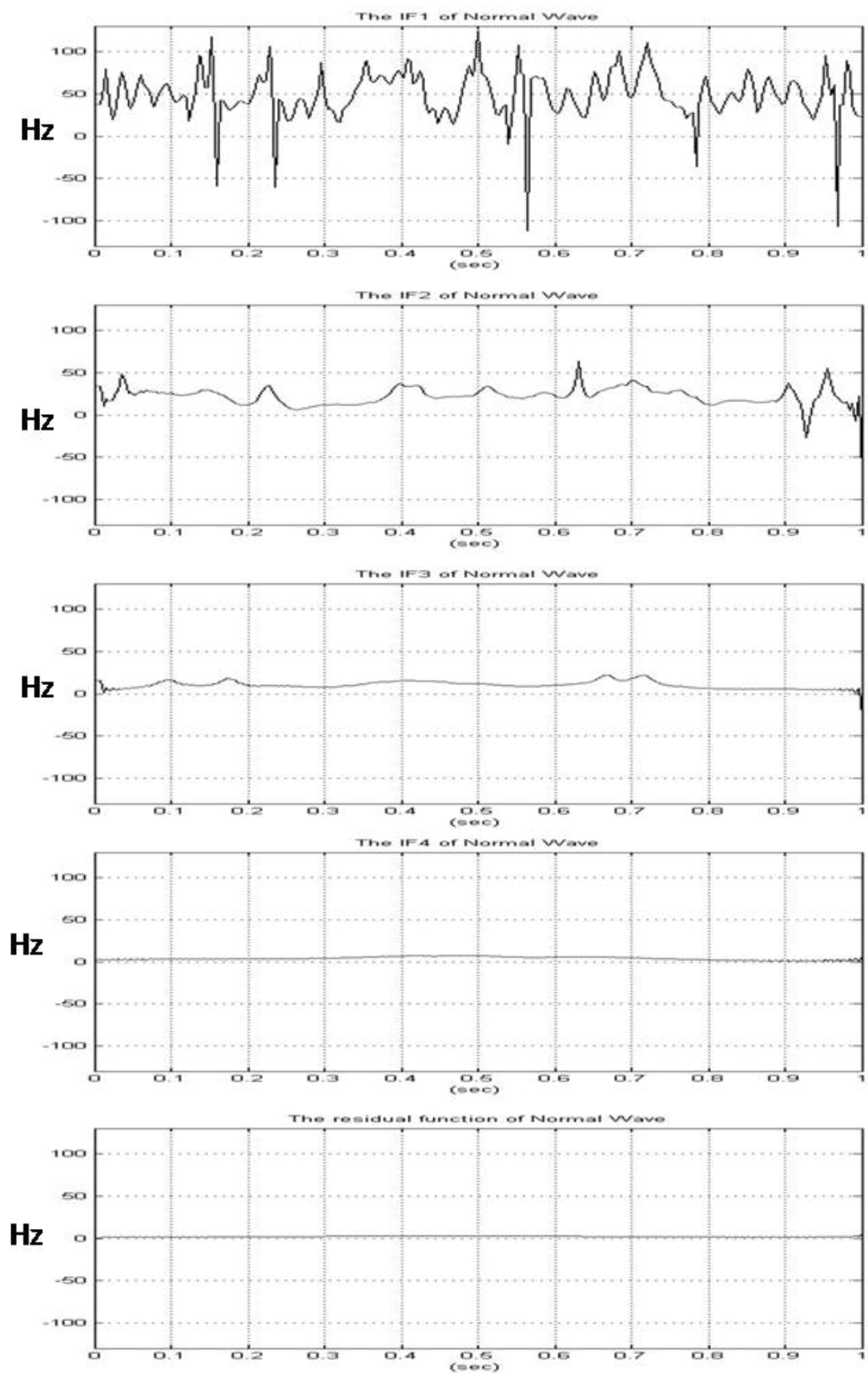Fig. 5. IFs of the sharp wave with a transmission BER of 10^{-7}.

Fig. 6. IFs of the normal wave with a transmission BER of 10^{-7}.

	Mean (uv)	Std (uv)	Max (uv)	Min (uv)	Eng (uv^2)	Eng (%)
sharp wave	1.95	22.72	76.64	-46.22	123340	100
IMF1	0.02	2.2	8.35	-11.07	1208.3	0.98
IMF2	-0.71	9.06	31.84	-27.68	20604	16.7
IMF3	0.79	13.08	29.55	-32.98	42764	34.67
IMF4	0.95	12.87	18.05	-19	41510	33.75
residual function	0.89	8.27	10.47	-15.57	17256	13.99

Table 1. Statistical characteristics of the sharp wave IMFs with a transmission BER of 10^{-7}.

	Mean (uv)	Std (uv)	Max (uv)	Min (uv)	Eng (uv^2)	Eng (%)
normal wave	-0.48	8.53	20.70	-10.60	20499	100
IMF1	0.02	1.08	2.67	-2.75	293.8	1.43
IMF2	0.14	2.32	7.65	-8.49	1349.2	6.57
IMF3	-0.36	2.98	7.07	-8.13	2253.3	10.99
IMF4	-0.62	5.93	11.65	-9.16	8877.8	43.31
residual function	-0.02	5.57	8.02	-7.90	7726.9	37.69

Table 2. Statistical characteristics of the normal wave IMFs with a transmission BER of 10^{-7}.

	Mean (Hz)	Std (Hz)	Max (Hz)	Min (Hz)
IF1	42.04	34.37	116.40	-121.49
IF2	16.25	12.55	106.70	-41.33
IF3	4.89	7.52	42.84	-43.76
IF4	1.94	0.73	3.75	0.23
residual function	0.91	0.67	8.6	-0.16

Table 3. Statistical characteristics of the sharp wave IFs with a transmission BER of 10^{-7}.

	Mean (Hz)	Std (Hz)	Max (Hz)	Min (Hz)
IF1	49.04	28.28	124.40	-112.08
IF2	21.96	11.57	63.22	-75.62
IF3	10.10	4.83	22.04	-26.8
IF4	3.93	1.90	7.48	0.52
residual function	2.04	0.55	5.53	0.05

Table 4. Statistical characteristics of the normal wave IFs with a transmission BER of 10^{-7}.

IMF3	<0.5Hz	δ	θ	α	β	γ
sharp	0.31	16497.95	25374.79	381.41	509.35	0.17
Normal	773.28	1336.66	117.95	25.45	0.00	0.00
sharp (%)	0.00	38.58	59.34	0.89	1.19	0.00
normal (%)	34.32	59.32	5.23	1.13	0.00	0.00

Table 5. Frequency-energy distributions of IMF3 of the sharp and normal waves with a transmission BER of 10-7.

IMF4	<0.5Hz	δ	θ
sharp	663.00	40853.00	0.00
normal	0.00	7696.00	1580.89
sharp(%)	1.60	98.40	0.00
normal(%)	0.00	82.20	17.80

Table 6. Frequency-energy distributions of IMF4 of the sharp and normal waves with a transmission BER of 10^{-7}.

residual function	<0.5Hz	δ	θ
sharp	2356.10	14421.09	236.54
normal	3.73	7714.66	8.52
sharp(%)	13.65	83.57	1.37
normal(%)	0.05	99.84	0.11

Table 7. Frequency-energy distributions of the residual function of the sharp and normal waves with a transmission BER of 10^{-7}.

sharp IMF3 (sec)	<0.5 Hz	δ	θ	α	β	γ
0-0.1	0.31	5.63	4.51	21.60	0.23	0
0.1-0.2	0	0.20	0	76.66	25.07	0.06
0.2-0.3	0	0	2217.07	41.63	0	0
0.3-0.4	0	11983.3	96.602	0	0	0
0.4-0.5	0	3264.05	8076.35	0	0	0
0.5-0.6	0	0	11104.50	0	0	0
0.6-0.7	0	427.44	3022.18	0	0	0
0.7-0.8	0	166.66	741.86	0	0	0
0.8-0.9	0	3.88	22.00	9.85	1.99	0.11
0.9-1.0	0	646.75	89.73	231.66	482.06	0

Table 8. Time-frequency-energy distributions of IMF3 of the sharp waves with a transmission BER of 10^{-7}.

sharp IMF4 (sec)	<0.5Hz	δ
0-0.1	0	4429.30
0.1-0.2	0	6789.34
0.2-0.3	0	1288.18
0.3-0.4	0	6003.27
0.4-0.5	0	1870.42
0.5-0.6	0	5935
0.6-0.7	0	1232.43
0.7-0.8	0	6105.55
0.8-0.9	0	5429.43
0.9-1.0	662.79	1764.27

Table 9. Time-frequency-energy distributions of IMF4 of the sharp waves with a transmission BER of 10^{-7}.

Normal IMF4 (sec)	δ	θ
0-0.1	1940.13	0
0.1-0.2	1125.07	0
0.2-0.3	1429.04	17.67
0.3-0.4	0	409.96
0.4-0.5	0	201.27
0.5-0.6	0	239.73
0.6-0.7	0	401.12
0.7-0.8	188.11	158.76
0.8-0.9	1056.87	0
0.9-1.0	1557.65	152.39

Table 10. Time-frequency-energy distributions of IMF4 of the normal waves with a transmission BER of 10^{-7}.

normal residual function (sec)	<0.5Hz	δ
0-0.1	3.73	523.16
0.1-0.2	0	1348.84
0.2-0.3	0	358.32
0.3-0.4	0	1045.06
0.4-0.5	0	439.20
0.5-0.6	0	1229.81
0.6-0.7	0	329.76
0.7-0.8	0	1138.58
0.8-0.9	0	1169.23
0.9-1.0	0	132.69

Table 11. Time-frequency-energy distributions of the residual function of the normal waves with a transmission BER of 10^{-7}.

4. Discussion

Hilbert-Huang transformation (HHT) is one of the major time-frequency analysis methods and is suitable for the analysis of local time signals. In this article, we use HHT-based method to analysis the signal deemed of the sharp wave. In addition, we describe the features of a sharp wave recorded and a normal wave recorded with a transmission bit error rate (BER) of 10^{-7} for patients with epilepsy by using HHT analysis method. Simulation results shows that the performance of the sharp wave based HHT time-frequency characteristics is not affected under the transmission BER of 10^{-7} assumptions. We present the intrinsic mode functions (IMF), instantaneous frequencies (IF), time-frequency-energy distributions for the sharp and normal waves. Clear energy-frequency-time variations of the sharp waves and normal waves with a transmission BER of 10^{-7} are shown. There are 4 IMFs and a residual function of the sharp and normal waves by using the HHT analysis. Analysis results show that the ratio of the energy of a sharp wave with the IMF3 and the total energy of a sharp wave, the ratio of the energy of a sharp wave with the IMF4 and the total energy of a sharp wave, the ratio of the energy of a normal wave with the IMF4 and the total energy of a normal wave, the ratio of the energy of a normal wave with the residual function and the total energy of a normal wave are 34.55%, 33.73%, 43.25%, and 37.63%, respectively. The ratio of the energy of the IMF4 of a sharp wave with δ (0.5Hz-4Hz) band and the total energy of the IMF4 of a sharp is 98.4%. The ratio of the energy of the IMF4 of a normal wave with δ (0.5Hz-4Hz) band and the total energy of IMF4 of a sharp is 82.2%. The mean IF of the IMF4 of a sharp wave is smaller than the mean IF of the IMF4 of a normal wave. From these analysis results, we observe that the HHT-based time-frequency characteristics of the sharp waves with a transmission BER of 10^{-7}.

5. Conclusion

The HHT-based time-frequency analysis approaches are suitable for studying the local and non-stationary normal waves and sharp waves in EEGs for epilepsy. We obtained the IMFs, and IFs to analyze the energy-frequency-time distributions of normal waves and sharp waves with a transmission BER of 10^{-7} in the EEG. The mean IF of IMF4 of a sharp wave is smaller than the mean IF of IMF4 of a normal wave. In addition, the substantial energies of IMF3 of the sharp wave are the δ band in the interval of 0.3-0.5 s, and the θ band in the interval of 0.4-0.7 s. The substantial energies of IMF4 of the sharp wave are the δ band in the intervals of 0.1-0.2 s, 0.3-0.4 s, and 0.7-0.9 s. In contrast, the substantial energies of IMF4 of the normal wave are the δ band in the intervals of 0-0.1 s, 0.1-0.3 s, and 0.8-1 s. The substantial energies of the residual function of the normal wave are the δ band in the intervals of 0.1-.0.2 s, 0.3-0.4 s, 0.5-0.6 s, and 0.7-0.9s. These observations show that the sharp signal characteristics and the IMFs, IFs, time-frequency-energy distributions of sharp-related and normal signals can be distinguished from each other, thereby ensuring more accurate diagnosis of patients with an epilepsy-related sharp.

6. Acknowledgements

7. References

Huang, N. E.; Shen, Z.; Long, S. R.; Wu, M. C.; Shih, H. H.; Zheng, Q.; Yen, N. C.; Tung C. C. & Liu, H. H. (1998). The empirical mode decomposition and the Hilbert spectrum for non- linear and non-stationary time series analysis. *Proceedings of the Royal Society of London Series A – Mathematical Physical and Engineering Sciences,* 903-995.

Yan, R. & Gao R. X. (2007). A tour of the Hilbert-Huang transform: an empirical tool for signal analysis. *IEEE Instrumentation & Measurement Magazine,* 11-15.

Cohen, L. (1989). Time-frequency distributions-a review. *I Proceedings of the IEEE,* 941–981.

Blanco, S.; Kochen, S.; Rooso, O. A.& Salgado, P. (1997). Applying time-frequency analysis to seizure EEG activity. *IEEE Engineering in Medicine and Biology,* 64-71.

Tzallas, A. T.; Tsipouras, M. G. & Fotiadis, D. I. (2009). Epileptic seizure detection in EEGs using time-frequency analysis. *IEEE Trans. Information Technology in Biomedicine,* 703-710.

Exarchos, T. P.; Tzallas, A. T.; Fotiadis, D. I.; Konitsiotis, S. & Giannopoulos, S. (2006). EEG transient event detection and classification using association rules. *IEEE Trans. Inf. Technol. Biomed,* 451–457.

Williams, W. J.; Zaveri, H. P. & Sackellares, J. C. (1995). Time-frequency analysis of electrophysiology signals in epilepsy. *IEEE Eng. Med. Biol,* 133–143.

Sharabaty, H.; Martin, H. J.; Jammes, B. & Esteve, D. (2006). Alpha and theta wave localisation using Hilbert-Huang transform: empirical study of the accuracy, *Proceedings of IEEE Int. Conf. Information and Communication Technologies,* 1159-1164.

Wang, L.; Xu, G.; Wang, J.; Yang, S. & Yan, W. (2008). Application of Hilbert-Huang transform for the study of motor imagery tasks, *Proceedings of IEEE Int. Conf. EMBS*, 3848-3851.

Wang, Y. L.; Liu, J. H. & Liu, Y. (2008). Automatic removal of ocular artifacts from electroencephalogram using Hilbert-Huang transform, *Proceedings of IEEE Int. Conf. ICBBE,*2138-2141.

Lin, C. F.; Chang, W. T.; Lee, H. W. & Hung, S. I. (2006). Downlink power control in multi-code CDMA mobile medicine system. *Medical & Biological Engineering & Computing,* 437-444.

Lin, C. F.; Chang, W. T. & Li, C. Y. (2007). A chaos-based visual encryption mechanism in JPEG2000 medical images. *J. of Medical and Biological Engineering,* 144-149.

Lin, C. F. & Chang, K. T. (2008). A power assignment mechanism in Ka band OFDM-based multi-satellites mobile telemedicine. *J. of Medical and Biological Engineering,* 17-22.

Lin, C. F. & Li, C. Y. (2008). A DS UWB transmission system for wireless telemedicine. *WSEAS Transactions on Systems*, 578-588.

Lin, C. F.; Chung, C. H.; Chen, Z. L.; Song, C. F. & Wang, Z. X. (2008). A chaos-based unequal encryption mechanism in wireless telemedicine with error decryption. *WSEAS Transactions on Systems,* 49-55.

Lin, C. F.; Chen, J. Y.; Shiu, R. H. & Chang, S. H. (2008). A Ka band WCDMA-based LEO transport architecture in mobile telemedicine, In: *Telemedicine in the 21st Century,* Lucia Martinez and Carla Gomez, (Ed.), 187-201, Nova Science Publishers, USA.

Lin, C. F.; Chung, C. H. & Lin, J. H. (2009). A Chaos-based visual encryption mechanism for EEG clinical signals. *Medical & Biological Engineering & Computing,* 757-762.

Lin, C. F. (2010). An Advance Wireless Multimedia Communication Application: Mobile Telemedicine. *WSEAS Transactions on Communications,* 206-215.

Lin, C. F.; Hung, S. I.; & Chiang, I. H. (Online First). 802.11n WLAN Transmission Scheme for Wireless Telemedicine Applications. *Proceedings of the Institution of Mechanical Engineers, Part H, Journal of Engineering in Medicine.*

Lin, C. F. (Online First). Mobile Telemedicine:A Survey Study. *Journal of Medical Systems.*

Lin, C. F. & Wang, B. S. H. (Accept). A 2D Chaos-based Visual Encryption Scheme for Clinical EEG Signals. *Journal of Marine Science and Technology.*

Lin, C. F.; Yeh S. W.; Peng, T. I.; Chien, Y. Y.; Wang, J. H. & Chang, S. H. (2008). A HHT-based time frequency analysis scheme in clinical alcoholic EEG signals. *WSEAS Transactions on Biology and Biomedicine,* 249-260.

Lin, C. F.; Yeh, S. W.; Chang, S. H.; Peng, T. I & Chien, Y. Y. (2010). An HHT-based time-frequency scheme for analyzing the EEG signals of clinical alcoholics. In: *Advances in Medicine and Biology, Volume 11,* Leon V. Berhardt, (Ed.), Nova Science Publishers, USA.

Lin, C. F.; Yeh, S. W.; Chang, S. H.; Peng, T. I & Chien, Y. Y. (2010). *An HHT-based Time-frequency Scheme for Analyzing the EEG Signals of Clinical Alcoholics,* Online Book, Nova Science Publishers, USA.
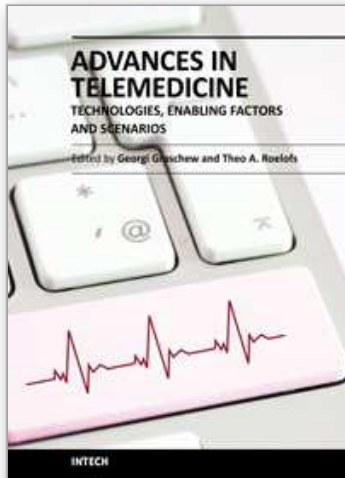
Advances in Telemedicine: Technologies, Enabling Factors and Scenarios

Edited by Prof. Georgi Graschew

Innovative developments in information and communication technologies (ICT) irrevocably change our lives and enable new possibilities for society. Telemedicine, which can be defined as novel ICT-enabled medical services that help to overcome classical barriers in space and time, definitely profits from this trend. Through Telemedicine patients can access medical expertise that may not be available at the patient's site. Telemedicine services can range from simply sending a fax message to a colleague to the use of broadband networks with multimodal video- and data streaming for second opinioning as well as medical telepresence. Telemedicine is more and more evolving into a multidisciplinary approach. This book project "Advances in Telemedicine" has been conceived to reflect this broad view and therefore has been split into two volumes, each covering specific themes: Volume 1: Technologies, Enabling Factors and Scenarios; Volume 2: Applications in Various Medical Disciplines and Geographical Regions. The current Volume 1 is structured into the following thematic sections: Fundamental Technologies; Applied Technologies; Enabling Factors; Scenarios.

INTECH
open science | open minds